

# Integration of Ground Truth Data via Cloud Computing for Enhanced Burn Severity Mapping – An Example from Honduras

Alexander Ariza<sup>1</sup>, Hannah Kemper<sup>2</sup> and Gerhard Kemper<sup>2</sup>

<sup>1</sup>UN Spider Bonn, Germany

<sup>2</sup>GGS GmbH Speyer, Germany

## Abstract

Until now, most severity products are generated from a reclassification of dNBR index ranges. In this study, we focused on an automated global burn severity mapping approach. Using the catalogue of satellite imagery and the high-performance computing power of GoogleEarthEngine we propose an automated pipeline to generate severity maps of burned areas at a medium scale of 30 and 10m from the time series of Landsat and Sentinel2 images. Landsat-8 images available during 2020 and the dNBR spectral index were used to calculate the severity level of each pixel using a calibration model and linear regression adjustments, which were taken in the field from the CBI index in an app developed for field capture. A calibration approach was carried out to give the severity level of the final burned areas after several carefully designed logic filters on the normalized burn rate (NBR). This script focuses on the fires that occurred in Honduras in 2020. The regression model found a similar spatial distribution and strong correlation between the areas analyzed in the field and those generated from the dNBR. The preliminary global validation showed that the overall accuracy reached 53.85%. However, the adjustments through the correlation models improved the results, yielding an  $R^2$  of 0.93 for the quadratic model, 0.79 for the Exponential model and 0.72 for the linear model.

**Keywords:** burn severity, Composite Burn Index (CBI), GEE, disaster management, regression models

## 1 Introduction

Accurately mapping burned areas is essential for quantifying carbon budgets (Chuvieco et al., 2018; Padilla et al., 2015) and for analyzing the relationship between vegetation and climate. It is needed to assess the impacts of fire as a land management tool and quantify trends and patterns in fire occurrence, among other relevant applications. Digital image processing aiming to map fire activities has been applied to a variety of images from sensors of various spatial, temporal, and spectral resolutions (Alonso-Canas and Chuvieco, 2015; Chuvieco et al., 2018). Considering the computational power of Google Earth Engine (GEE) it is a powerful tool to enhance image preprocessing and algorithm application to big datasets. Common datasets used for image classification, burn severity detection or change detection in GEE are Landsat (Long

et al., 2019), MODIS or Sentinel-1 radar imagery. Analyses experienced a major improvement using (semi-)automatic image classification and thus are based on a greater database of thousands of images. Implementing new algorithms from Machine Learning for image classification and damage detection, big steps towards an automated burn severity workflow have been taken (Parks et al., 2018). Nevertheless, all these remote sensing data workflows show difficulties in integrating ground truth data to validate the created results. One of the major shortcomings in remote sensing image processing is that several common techniques use validation with reference images (Parks et al., 2018). Further, it is crucial to integrate ground truth data from the field into the methodology. This is enabled considering the power of Citizen Science and modern web applications like EpiCollect, which allows bi-directional communication between workers in the field and the image repository of their project (Ananensen et al., 2019). Regarding the applicability of EpiCollect in the field of Geosciences and Remote Sensing, the advantages of real-time ground truth data for validation of computed results are apparent (Hoffmann et al., 2016).

## **2 Area of Study**

The Central Forest Corridor region is located in the centre of Honduras. It has a size of 186,525 ha and is delimited to safeguard water-producing areas of 13 municipalities.

## **3 Methodology**

In this study, the limits of the severity map were defined by the spatial extent of the Central American fires in spring 2020. The resolution of the severity products was 30 and 10 m. The severity mapping of the burned area through GEE is described in Figure 1.

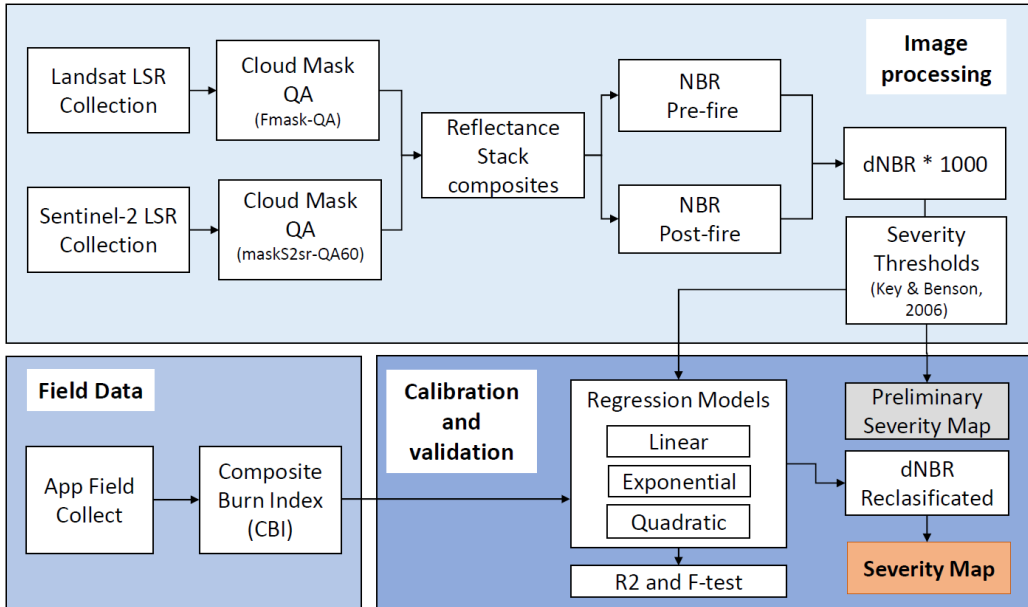


**Figure 1:** Workflow from image processing (chapter 3.1), field data (chapter 3.2) and model calibration and validation (chapter 3.3)

As shown in Figure 1, the pipeline consisted mainly of three steps: model training, per-pixel processing and modelling of the burned area.

### 3.1 Datasets and Image processing

We produced fire severity metrics for the study area in GEE based on the Landsat 8 and Sentinel 2 Surface Reflectance. The data has been corrected atmospherically using the Land Surface Reflectance Code (LaSRC)<sup>1</sup>, which uses the quality assurance (QA) layers, which are produced during the atmospheric correction process, to estimate the amount of high aerosol that impact the derived surface reflectance. The clouds were masked using FMask (Zhu & Woodcock, 2014) as well as a per-pixel saturation mask in Landsat images, and the maskS2sr function based on the Sentinel 2 band 'QA60' the correction was concluded.

In this phase, we generate Landsat and Sentinel composites for the cloudless dates before the fire (from 06 to 30 March) and after the fire (from 15 to 17 April) using a pixel-based approach within the GEE platform, and then we reduce pixel unmasking in the reflectance stack composite using pre-and post-fire "mosaic". Then, we calculated spectral transformations in order to enhance the discrimination of changes in the land surface. In this study, we calculated two

<sup>1</sup><https://www.usgs.gov/media/files/landsat-8-collection-1-land-surface-reflectance-code-product-guide>

spectral transformations, the Normalized Burn Ratio (Formula 1), which contrasts the difference in reflectance between the NIR and the SWIR-2 (Short Wave Infrared), and the temporal index version dNBR (Formula 2) (Miller et al., 2007). We calculated spectral transformations in order to enhance the discrimination of changes in the land surface.

$$NBR = \left( \frac{NIR - SWIR}{NIR + SWIR} \right)$$

Formula 1: Normalized Burn Ratio

$$dNBR = (NBR_{prefire} - NBR_{postfire}) \times 1000$$

Formula 2: Differential Normalized Burn Ratio

The dNBR shows the best contrast between healthy photosynthetic vegetation and burnt vegetation. This index, similarly to NDVI, has values between -1 and 1, but it was multiplied by 1000 in order to manage the data type (integer) better, to follow the convention established by Key and Benson (2006). Therefore, higher values above 100 dNBR are set as the "burnout" threshold. In the same way, the dNBR can be used to assess the severity of burns, as areas with higher dNBR values indicate more serious damage. In contrast areas with negative dNBR values may show higher vegetation productivity. dNBR can be classified according to the ranges of severity of burns. The thresholds of severity levels used in this study were those proposed by the United States Geological Survey (USGS), in this case, the class marks of the unburned to high ranges of the Key and Benson (2006) classification were used. These dNBR thresholds thus establish the respective fire severity classes (Table 1).

**Table 1:** Thresholds of severity levels from dNBR index

Severity Level	dNBR Range (scaled by $10^3$ )	dNBR Range (not scaled)
Enhanced Regrowth, high (post-fire)	-500 to -251	-0.500 to -0.251
Enhanced Regrowth, low (post-fire)	-250 to -101	-0.250 to -0.101
Unburned	-100 to +99	-0.100 to +0.99
Low Severity	+100 to +269	+0.100 to +0.269
Moderate-low Severity	+270 to +439	+0.270 to +0.439
Miderate-high Severity	+440 to +659	+0.440 to +0.659
High Severity	+660 to +1300	+0.660 to +1.300

### 3.2 Field data

The field data represents the composite burn index (CBI) (Key and Benson, 2006), which rates factors such as surface fuel consumption, soil char, vegetation mortality, and scorching of trees. CBI is rated on a continuous scale from zero to three, with CBI = 0 reflecting no change and CBI = 3 reflecting the highest degree of fire-induced ecological change.

The field data were collected using EpiCollect, a tool developed in 2009 by the Imperial College London research group, which allows taking and sending georeferenced information from phones to a central website. The information there is analyzed graphically and filtered according to the variables, using Google Maps/Earth. The stored data can be downloaded and viewed directly on the phone in Google Maps. The tool to capture field data is available here: (<https://five.epicollect.net/project/cbi>).

### 3.3 Severity calibration model

We aimed to determine whether our GEE based methodology (the calibration by regression models via CBI method) produced Landsat-based fire severity datasets with equivalent or higher validation statistics than severity datasets produced using one pre-fire and one post-fire scene (i.e., the standard approach since these metrics were introduced).

This calibration has two components, first the result of the dNBR index classified into five severity intervals (Carl and Key, 2006), and second the CBI field index which relies on 13 field-plots covering the research area, with a homogenean distribution per every severity class. Of the 13 field-based CBI plots, 23% are considered not burnt, (CBI=0), low severity (CBI <1.0) 23%, moderate-low severity (CBI 1.0 and <1.5) 8 %, moderate-high severity (CBI 1.5 and <2.0) 23 %, and 23% are high severity (CBI >2.0).

(Figure 2).

After, we evaluated the global accuracy of preliminary classification through the confusion matrix. Subsequently, the dNBR values were adjusted through regression analysis by three different models (linear, exponential and quadratic), evaluated through an ANOVA test in order to determine how well each model fits the field data. Using the SPSS tool, a variety of goodness-of-fit statistics are presented, using the value of R squared ( $R^2$ ), and the statistic F. Finally, we extracted GEE-derived dNBR, values based on spatial analysis and then applied linear regression through statistic reducer function "ee.Reducer.linearRegression", to evaluate the performance of each severity metric. Specifically, we quantified the correspondence of each severity metric (the dependent variable) to CBI (the independent variable) as the coefficient of determination, which is the  $R^2$  of a linear regression between predicted and observed severity values.

We conducted this analysis for the fire study area and reported  $R^2$  values. We then conducted a parallel analysis but used dNBR reclassify derived severity mapping. This parallel analysis allows a comparison of severity datasets produced using one pre-fire and one post-fire image (e.g., CBI-derived metrics) with the calibration by regression approach as with GEE.

## 4 Results and Analysis

Using GEE, we were able to produce dNBR quickly, and CBI including composite burned index on (specifically to calibration by regression method) for the 13 fields-plots analyzed; fire averaged about 237,40 hectares (Figure 2).

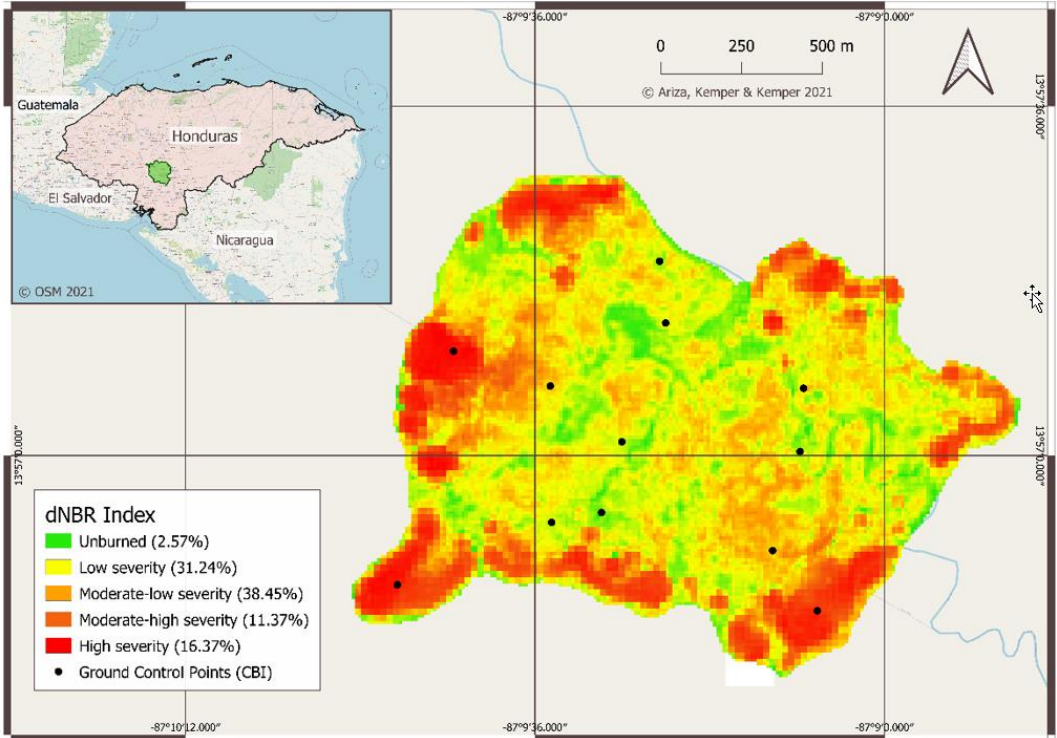


**Figure 2:** Severity mapping and location of the 13 CBI included in the calibration of the differential normalized burn ratio (dNBR). Tegucigalpa, Honduras

The entire process took approximately one minute, though this is a rough estimate that depends on the size and available resources shared with other users (Gorelick et al., 2017). Nonetheless, the processing time is quick with fairly low investment in terms of human labour.

The confusion matrix results showed the outcome of the preliminary classifier dNBR, with an overall accuracy of 53,8%. However, as can be seen in Table 2, the regression analysis results of  $R^2$ , the value of the F test, and its significance value for each of the three models are presented. Although the linear regression model presents a moderate value of  $R^2$  (0.87), its significance value F is the highest (83.58), while the quadratic model with the highest value of  $R^2$  (0.93) presents a significance value of F minor (79.37), all models with a significance of 0.000, less than 0.05 which allows concluding that there is a significant relationship between the variables (dNBR and CBI), is much stronger in the linear and quadratic model.

**Table 2:** Regression Analysis Results of dNBR as dependent variable and CBI as an independent variable

Model Equation	Model summary					Parameter Estimates	
	R <sup>2</sup>	F	df1	df2	Sig	b1	b2
Linear	0.874	83.579	1	12	.000	332.757	139.751
Quadratic	0.935	79.376	2	11	.000	-7.299	
Exponential	0.729	32.218	1	12	.000	2.932	

The correspondence between CBI and each severity metric for 13 plots covering fire was evaluated simultaneously using the regression models; the adjust was consistently higher for the GEE-derived severity high and moderate class as compared to the unburned class (Figure 3).

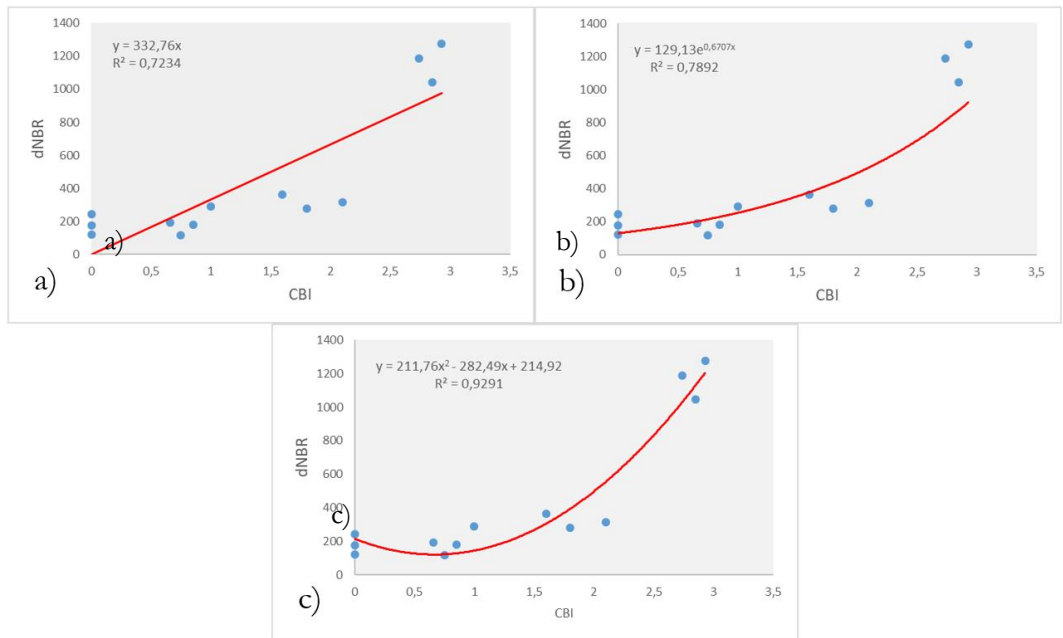


**Figure 3:** Regression models showing the correlation of CBI control points with dNBR. a) linear R<sup>2</sup>= 0.87; b) exponential R<sup>2</sup>=0.79; c) quadratic R<sup>2</sup> = 0.93

In general terms, the linear and quadratic models improve the fit of the severity mapping through the dNBR. Furthermore, the inclusion of the CBI increased the correspondence to field severity measure for the fire. In this case, all terms in the linear, exponential and quadratic regressions for severity metric were statistically significant ( $p < 0.05$ ).

## 5 Conclusions

This paper presented a practical and efficient methodology for producing one Landsat 8 and Sentinel 2 based fire severity metric: dNBR and specifically the calibration by regression CBI method. This method relies on Google Earth Engine and provides expanded potential in terms of fire severity monitoring and research in regions outside of Honduras that does not have a dedicated program for mapping fire severity. We aimed to evaluate differences between the GEE-based calibration by a regression of the CBI method approach to the standard approach in which one pre-fire and post-fire Landsat scene is used to produce severity datasets through the thresholds of severity levels from dNBR index. The inclusion of the CBI provided additional improvements in the class severity Thresholds definitions for fire severity mapping on GEE. This provides further evidence that the inclusion of the field data should be considered when multiple fires are of interest (Parks et al., 2018). In conclusion, the application of the different regression models (Linear, Quadratic and Exponential) under the test of general significance (F) is greater than their level of significance, which allows us to conclude that the application of the regression model (Linear and Quadratic) provides a better fit of the severity obtained by the CBI than the dNBR-only intercept model.

## Acknowledgement

Juan Carlos Villagran de Leon, programme officer head of UN-SPIDER Programme United Nations Office for Outer Space Affairs (UNOOSA); and Dáryl Medina Reyes from Forest Conservation Institute of Honduras (ICF).

## References

- Aanensen, D.; Huntley D.; Feil,E.; al-Own, F.; Spratt, B. 2009. EpiCollect: Linking Smartphones to Web Applications for Epidemiology, Ecology and Community Data Collection. *PLoS ONE* 4(9): e6968. doi:10.1371/journal.pone.0006968
- Alonso-Canas, Itziar, and Emilio Chuvieco. 2015. Global burned area mapping from ENVISAT-MERIS and MODIS active fire data. *Remote Sensing of Environment*.  
https://doi.org/10.1016/j.rse.2015.03.011.
- Chuvieco, Emilio, Joshua Lizundia-Loiola, Maria Lucrecia Pettinari, Ruben Ramo, Marc Padilla, Kevin Tansey, Florent Mouillot, et al. 2018. Generation and analysis of a new global burned area product based on MODIS 250 m reflectance bands and thermal anomalies. *Earth System Science Data*.  
https://doi.org/10.5194/essd-10-2015-2018.
- Gorelick, Noel, Matt Hancher, Mike Dixon, Simon Ilyushchenko, David Thau, and Rebecca Moore. 2017. Google Earth Engine: Planetary-scale geospatial analysis for everyone. *Remote Sensing of Environment*. https://doi.org/10.1016/j.rse.2017.06.031.
- Hoffmann, G. P., Borelli, R. M., I. J., Schmidt Nanni, A. (2018): “O uso de geotecnologias livres: QGIS e EpiCollect no levantamento de dados em geociências”, *GeoFocus (Artículos)*, nº 21, p. 39-55. ISSN: 1578-5157 http://dx.doi.org/10.21138/GF.504
- Key, C.H., Benson, N.C. 2006. Landscape Assessment (LA). In: Lutes, D.C., Keane, R.E., Caratti, J.F., Key, C.H., Benson, N.C., Sutherland, S., & Gangi, L.J. (eds). *FIREMON: Fire effects monitoring*



- and inventory system. USDA Forest Service, Rocky Mountain Research Station. Gen. Tech. Rep. RMRS-GTR-164-CD, 1-55.
- Long, T., Zhang, Z., He, G.; Jiao, W.; Tang, C.; Wu, B.; Zhang, X.; Guizhou, W.; Yin, R. 2019. 30 m Resolution Global Annual Burned Area Mapping Based on Landsat Images and Google Earth Engine. *Remote Sensing*. doi:10.3390/rs11050489
- Miller, Jay D., Eric E. Knapp, Carl H. Key, Carl N. Skinner, Clint J. Isbell, R. Max Creasy, and Joseph W. Sherlock. 2009. Calibration and validation of the relative differenced Normalized Burn Ratio (RdNBR) to three measures of fire severity in the Sierra Nevada and Klamath Mountains, California, USA. *Remote Sensing of Environment*. <https://doi.org/10.1016/j.rse.2008.11.009>.
- Padilla, Marc, Stephen V. Stehman, Ruben Ramo, Dante Corti, Stijn Hantson, Patricia Oliva, Itziar Alonso-Canas, et al. 2015. Comparing the accuracies of remote sensing global burned area products using stratified random sampling and estimation. *Remote Sensing of Environment*. <https://doi.org/10.1016/j.rse.2015.01.005>.
- Parks, Sean A.; Holsinger, Lisa M.; Voss, Morgan A.; Loehman, Rachel A.; Robinson, Nathaniel P. 2018. "Mean Composite Fire Severity Metrics Computed with Google Earth Engine Offer Improved Accuracy and Expanded Mapping Potential" *Remote Sens.* 10, no. 6: 879. <https://doi.org/10.3390/rs10060879>
- Zhu, Zhe, and Curtis E. Woodcock. 2014. Automated cloud, cloud shadow, and snow detection in multitemporal Landsat data: An algorithm designed specifically for monitoring land cover change. *Remote Sensing of Environment*. <https://doi.org/10.1016/j.rse.2014.06.012>.